Mechanistic Understanding and Metal Tuning as a Strategy for Improving Alkyl–Alkyl Cross-Coupling Catalysis with Early Transition Metals

Roman G. Belli, Victoria C. Tafuri, Courtney C. Roberts

University of Minnesota, Minneapolis, MN, 55455, USA

KEYWORDS (Word Style "BG_Keywords"). If you are submitting your paper to a journal that requires keywords, provide significant keywords to aid the reader in literature retrieval.

ABSTRACT: Alkyl–alkyl cross-coupling is a powerful C–C bond forming transformation typically catalyzed by late transition metals. Herein we report a mechanistic investigation into an early transition metal-catalyzed variant of this reaction. Through this mechanistic understanding, an ideal Y catalyst was determined through tuning of the metal in order to optimize for oxidation potential, the rate limiting step in this reaction. A wide substrate scope is revealed that includes a variety of functional groups as well as unactivated substrates.

Carbon–carbon bond forming cross-coupling is a powerful reaction for building up molecular complexity. This reaction is traditionally catalyzed using late transition metals such as Fe, Co, Ni, Cu, and Pd.[1–9] Optimization of these reactions to improve efficiency or expand the scope when catalyzed by late transition metals are often achieved through changing the ligand.[10] For example, recent reports by Sigman and Doyle demonstrate the impact that even subtle steric and electronic changes in phosphine ligands can have on the success of metal-catalyzed reactions (**Figure 1a**).[11] Ligand tuning is the state-of-the-art optimization tool in large part due to the variety of cross-couplings mechanisms that can be accessed and that the operative mechanism is highly dependent on the metal. It also has drawbacks as ligands can take multiple steps to prepare. A complementary approach to catalyst development would be to use a single ligand framework that could be screened for optimal reactivity in catalysis by simply changing the metal, the final step in catalyst modification (**Figure 1b**). This would align with principles established in medical chemistry which encourage the point of diversification to be as late stage as possible.[12,13]

The diagonal periodic relationships of the early transition metals (i.e. Sc, Zr and Ta) are well-established which demonstrates that the similar reactivity is not only limited within a group, but also across groups containing d^0 metals.[14] This identifies early transition metals as ideal candidates to test in the pursuit of metal tuning for improvements in cross-coupling. Unfortunately, cross-coupling is not traditionally catalyzed by early transition metals because they typically exist in the d^0 state which means they lack the electrons necessary to undergo oxidative addition and render reductive elimination challenging.[15] By using a redox-active ligand[16–22], which can undergo oxidation and reduction in place of the metal, we successfully utilized a tris(amido)Sc complex (**1**) in the catalytic cross-coupling of benzylic bromides with alkyl zinc reagents for the first time.[23] Both the electrophilic and nucleophilic coupling partners contained substrates with β-hydrogens that were well tolerated, an

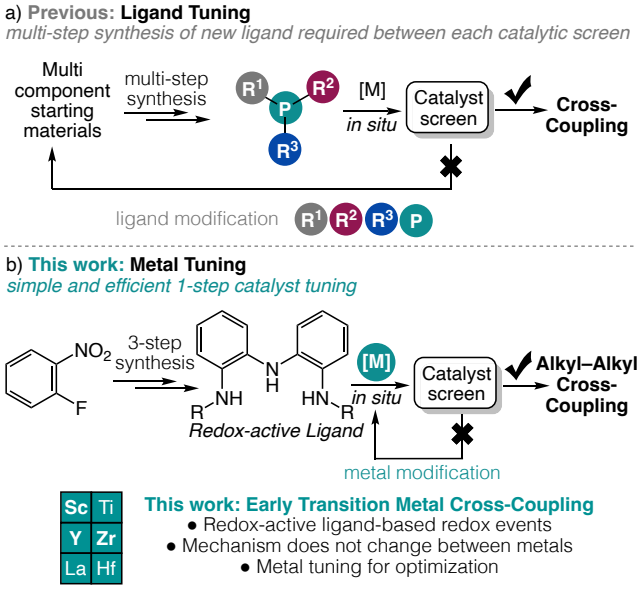

Figure 1. a) Ligand tuning, b) This work: metal tuning for catalyst optimization for alkyl–alkyl cross coupling

advantage over many late transition metal-catalyzed systems. Through use of a redox-active ligand to facilitate the redox events and principles of diagonal relationships and periodic trends, we hypothesized that changing the d^0 metal would allow us to improve the reactivity of the system as well as expand the scope. Herein, we explore the mechanism of this new reaction in order to support the claim that changing the metal can tune reactivity due to identifying the rate determining step. We demonstrate that through metal tuning using a single tris(amido) ligand with Sc, Y, and Zr we were able to identity a more active and general catalyst for d^0 metal-catalyzed cross-coupling. Guided by this mechanistic study, we also report the use of

photochemistry to expand the scope of this reaction even further to include unactivated alkyl electrophiles.

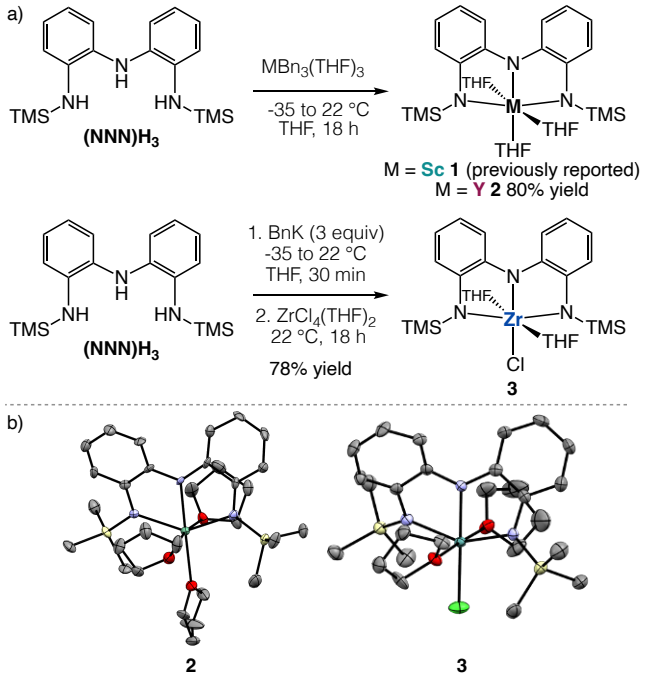

Figure 2. a) Synthesis of **1**, **2**, and **3**, b) crystal structures of **2** and **3**

First, the Y and Zr analogs of our previously reported Sc complex **1** were prepared (**Figure 2b**) in order to explore the relationships both diagonal and below Sc.[23] Complex **2** was isolated as a yellow solid via the addition of $(NNN)H_3$ to $YBn_3(THF)_3$ in THF at −35 °C, a similar method to our previously reported procedure to prepare **1**. Deprotonation of $(NNN)H_3$ with benzyl potassium followed by the addition of $ZrCl_4THF_2$ at −35°C in THF afforded complex **3** as an orange solid. The ^{1}H NMR spectra of **2** and **3** in THF-d_8, show four

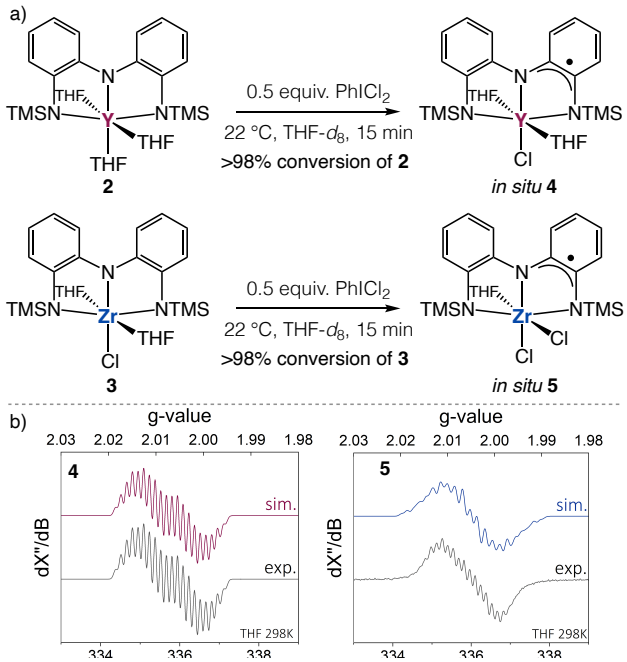

Figure 2. a) Chemical oxidation of **2** and **3**, b) EPR spectra of oxidized complexes **4** and **5**

aromatic protons and a single peak for the TMS groups of the ligand, indicative of the metalated ligand. Single crystals of **2**

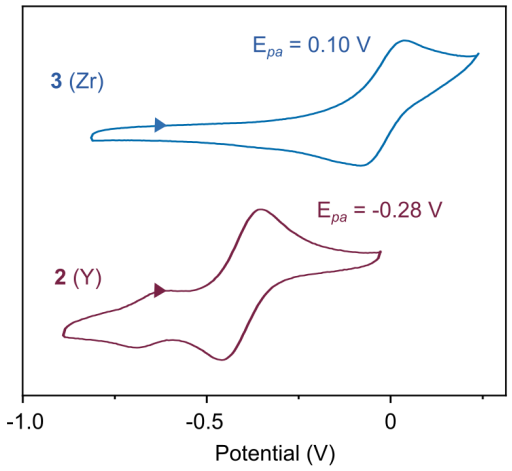

Figure 4. CVs of **2** and **3**

and **3** suitable for X-ray diffraction were grown from concentrated THF solutions with pentane vapour diffusion. The structures of **2** and **3** (**Figure 2b**) show that the geometry around the metal centers are pseudo-octahedral with the N-Y-N and N-Zr-N bond angles with the terminal Ns of 143.1° and 148.3°, respectively. The Y-N and Zr-N bond distances range from 2.252 to 2.325 Å and 2.122 to 2.149 Å, respectively. The smaller N1-M-N3 bond angle and M-N bond distances of **2** compared to **1** and **3** are consistent with the larger ionic radius of Y relative to Sc and Zr. The C–C and C–N bond distances in **2** and **3** are consistent with C–C double bonds and C–N single bonds, ranging from 1.375 to 1.433 and 1.395 to 1.411 Å respectively,

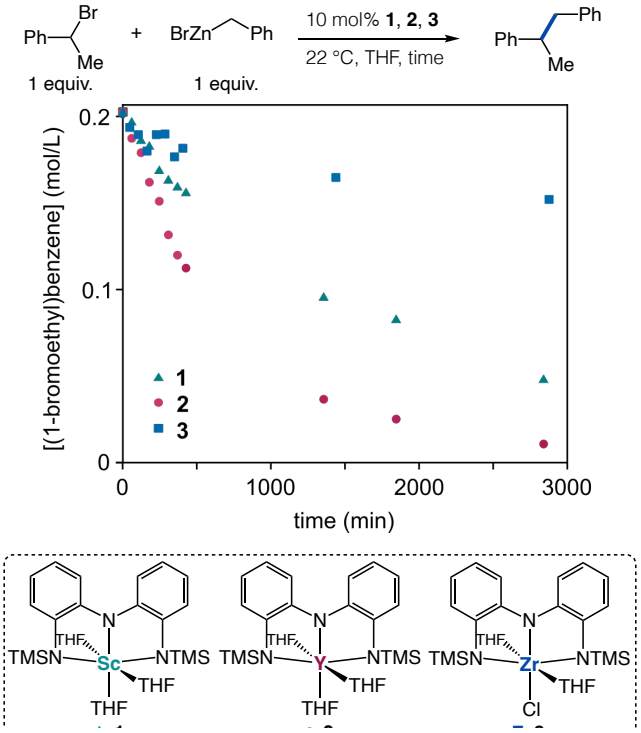

Figure 5. Monitoring cross-coupling reaction rates with **1**, **2**, and **3**

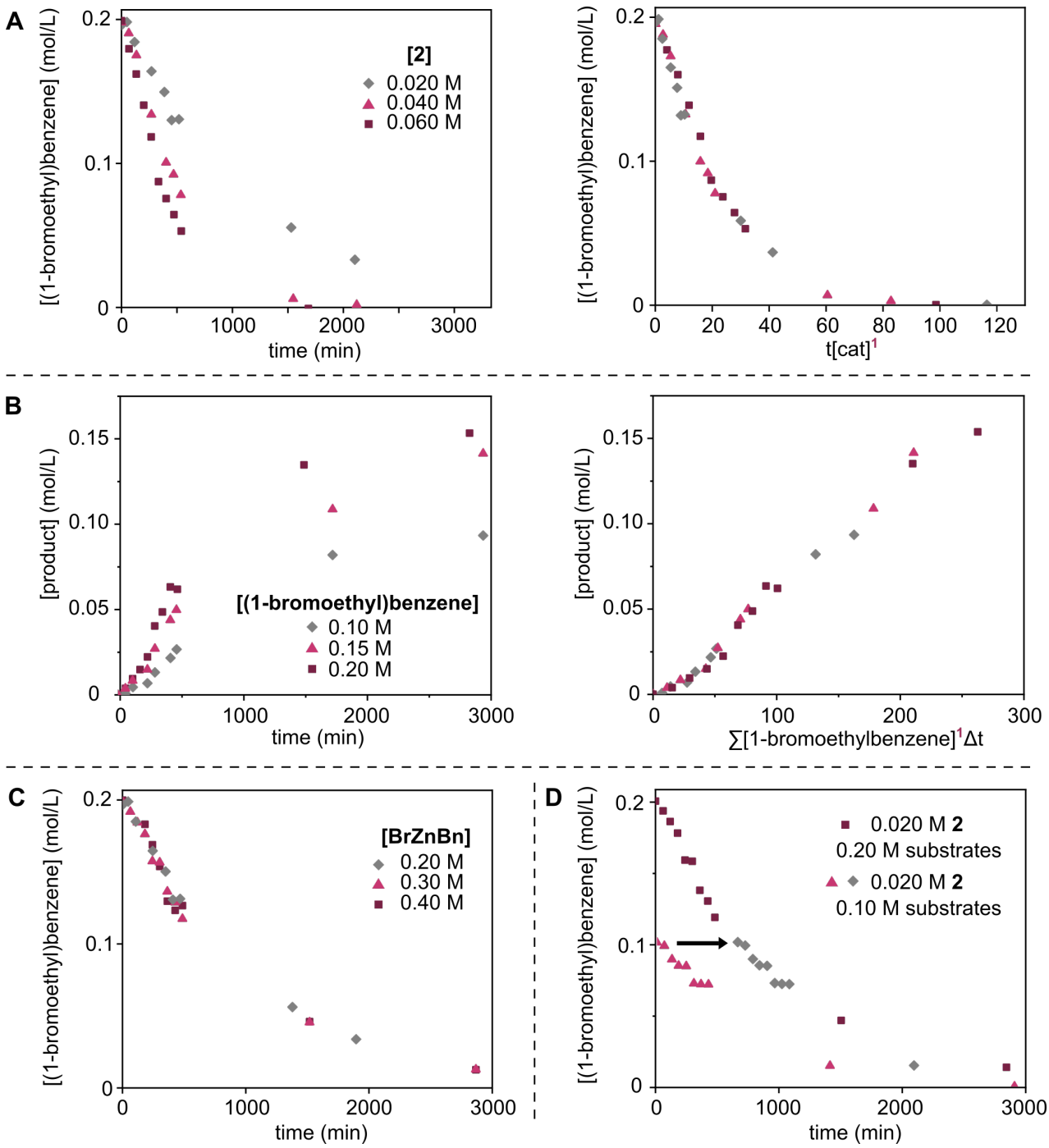

Figure 6. a) Determination of rate dependence on **2**, b) Determination of rate dependence on electrophile, c) Determination of rate dependence on nucleophile, d) Exploration of catalyst deactivation

which indicates the ligand is in a reduced state for both complexes.

Similar to **1**, complex **2** and **3** participate in one electron oxidation reactivity (**Figure 3a**). Addition of 0.5 equiv of $PhICl_2$ to **2** and **3** in THF-d_8 results in an immediate color change of the solutions from yellow to dark green or dark red, respectively. The ^{1}H NMR spectra of these reaction mixtures show the presence of PhI (byproduct of oxidation with $PhICl_2$) as well as a broad peak at ~ -0.6 and ~ -0.3 ppm that is assigned as the TMS peak of the resulting paramagnetic complexes (NNN•)YCl(THF)$_2$ (**4**) and (NNN•)$ZrCl_2$(THF) (**5**), respectively. The X-band EPR spectrum of **4** in fluid THF at 298 K displays a single isotropic signal with g_{iso} = 2.0218 (**Figure 3b**). Resolved hyperfine coupling to each nitrogen of the tris(amido) chelate (A_{iso}(^{14}N, n = 2) = 12.7 MHz ; A_{iso}(^{14}N, n = 1) = 15.3 MHz) as well as 3 aryl protons of the chelate (A_{iso}(^{1}H, n = 3) = 4.5 MHz) was observed. Superhyperfine coupling to the ^{89}Y nucleus (I = 1/2, 100% natural abundance) was also observed, with A_{iso} = 21.8 MHz. The X-band EPR spectrum of **5** in fluid THF at 298 K displays a single isotropic signal at with g_{iso} = 2.004 (**Figure 3b**). Resolved hyperfine coupling to each nitrogen of the tris(amido) chelate (A_{iso}(^{14}N, n = 2) = 9.2 MHz ; A_{iso}(^{14}N, n = 1) = 8.5 MHz) as well as 3 aryl protons of the chelate (A_{iso}(^{1}H, n = 3) = 3.6 MHz) was observed. Superhyperfine coupling to

the ^{91}Zr (I = 5/2, 11.22% natural abundance) was also observed, with A_{iso} = 6.2 MHz.

Electrochemical analysis of these three complexes shows that the oxidation potential (*Epa*) of **2** is lowest at -0.28 V, followed by **1** at -0.18 V[23] and **3** at 0.10 V (**Figure 4**). The oxidation of **1** is irreversible, which we previously established was due to an irreversible electron transfer. The oxidation of **2** and **3** are quasi-reversible as there is a slight dependence of the peak potential with respect to the scan rate (Supporting Information, Figure S5 and S12).[24] In addition, the peak currents for these oxidations are approximately equal. The difference in oxidation potentials of **1**-**3** may be due to a combination of the difference in electronegativities of these metals (Sc > Zr > Y) as well as the different oxidation states (M^{III} vs M^{IV}).

Next, the catalyst activity of **1**, **2**, and **3**, which all catalyze alkyl–alkyl cross-coupling of benzylic bromides and alkyl zinc bromides, was compared by monitoring the rate of consumption of the starting electrophile over time (**Figure 5**) in order to establish if, as we hypothesized, the rates of the reaction could be altered based on metal tuning. ^{1}H NMR monitoring of the catalytic cross-coupling of (1-bromoethyl)benzene with benzyl zinc bromide using 10 mol% of **1**, **2** and **3** shows that **2** is a more active catalyst than **1** with complex **3** being the least active catalyst (**Figure 5**). Y complex **2** results in the consumption of 95% of (1-bromoethyl)benzene within 48 h, whereas Sc complex **1** results in 76% consumption. With Zr complex **3** the reaction has only consumed 33% of the starting materials after 48 h. The higher activity of **2** relative to **1** and **3** is likely due to the fact that **2** has the lowest oxidation potential of these three complexes as demonstrated by CV studies. Homocoupled electrophile is a minor byproduct of the reaction but ratios of cross-coupled to homocoupled product do not change appreciably between catalysts.

The catalyst activity being correlated to the oxidation potential preliminarily points to oxidative addition being involved in the rate limiting step of the reaction. Variable time normalization analysis was used to determine the experimental rate expression for the cross-coupling of (1-bromoethyl)benzene with benzyl zinc bromide catalyzed by the most active catalyst **2** (**Figure 6**).[25–27] The reaction has a first order reaction rate dependence on the concentration of both **2** and (1-bromoethyl)benzene (**Figure 6**, A and B, respectively), with an overall rate expression of k[**2**][(1-bromoethyl)benzene]. The zero-order dependence on the concentration of benzyl zinc bromide (**Figure 6**, C) suggests that transmetallation occurs after the rate-limiting step. This supports that oxidative addition is the rate-limiting step of the proposed mechanism. A "same excess" experiment confirmed that catalyst deactivation does not occur during catalysis (**Figure 6**, D).[28,29] The good overlap of the kinetic profile of the reaction performed using half the initial substrate concentrations (▲) after time adjustment (◆) with the kinetic profile of the reaction with standard conditions (■) indicates no catalyst deactivation has occurred over the course of the reaction.

Previous studies with Sc implicated a radical intermediate in the oxidative addition step.[23] To further corroborate this with the Y analog of this catalyst, catalytic cross-coupling using complex **2** with *meta*- and *para*-substituted derivatives of (1-bromoethyl)benzene was investigated in order to probe a linear free energy relationship for this catalytic reaction (**Figure 7**). The decrease in the concentration of the (1-bromoethyl)benzene derivatives was monitored by ^{1}H NMR in order

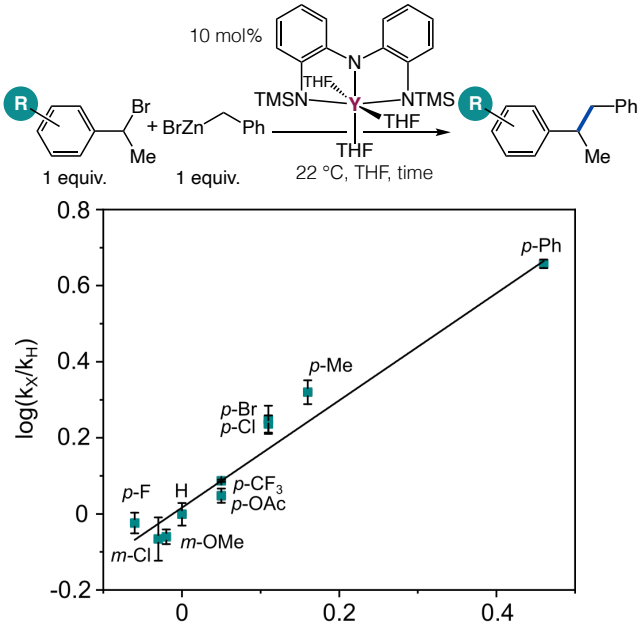

Figure 7. Creary plot for electronically different electrophiles

to obtain rate constants for these reactions. Plotting the log(k_X/k_H) with respect to Creary parameters revealed a linear relationship.[30] The Creary σ parameters take into account the ability of different substituents to stabilize radical intermediates (i.e. *p*-F is destabilizing and *p*-Ph is stabilizing for radicals). The linear relationship observed confirms that the mechanism for this cross-coupling catalyzed by **2** involves the intermediacy of a benzylic radical. This is in agreement with the previous mechanistic studies performed with Sc complex **1**, demonstrating that changing the d^0 metal did not alter this aspect of the mechanism. It is worth noting that plotting the log(k_X/k_H) with respect to the corresponding Hammett parameters did not give any clear trend (see Supporting Information, Figure S23), which rules out the formation of a negative or positive charge in the catalytic intermediates.

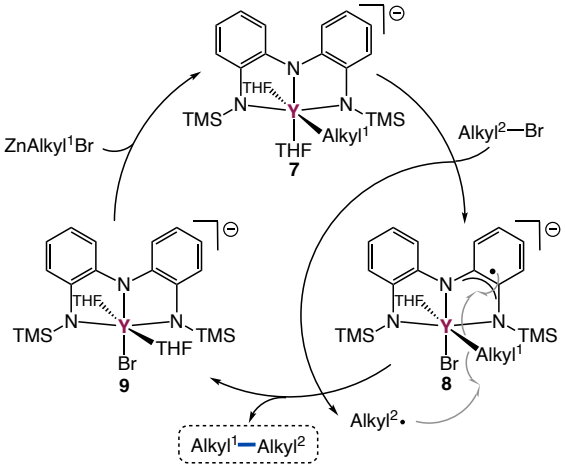

Figure 8. Proposed mechanism

Based on the experimental evidence, a proposed mechanism for cross-coupling catalyzed by complexes **1**-**3** is shown in Figure 8. First, transmetallation occurs between **2** and benzyl zinc bromide to afford **7**, an on-cycle catalytic intermediate. One electron oxidative addition via halogen atom abstraction from Alkyl^2–Br to **7** generates the paramagnetic complex

8 and Alkyl^2•. Attack of Alkyl^2• at Y–Alkyl^1 of **8** generates the cross-coupled product and **9**. Subsequent transmetallation regenerates **7**. Homocoupling of Alkyl^2• is also observed as an off-cycle process due to its outer-sphere formation.

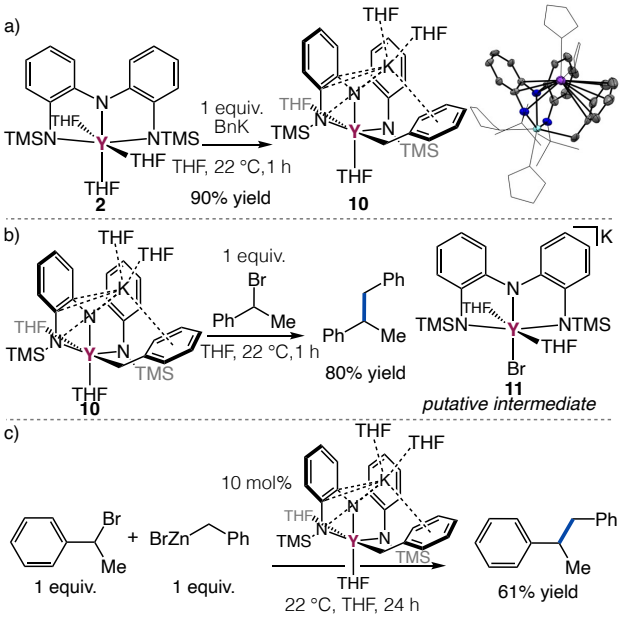

Figure 9. a) Independent synthesis of 10, the K analog of catalytic intermediate 7, b) Use of 10 in C–C bond formation, c) Use 10 as a catalyst

We wanted to further investigate the proposed mechanism by isolating proposed catalytic intermediates. A key intermediate in the proposed mechanism for this catalysis is **7**, which we propose forms via transmetallation between benzyl zinc bromide and **2**. The ^{1}H NMR spectrum in THF-d_8 of the addition of one equiv of benzyl zinc bromide to **2** shows that all the benzyl zinc bromide has been consumed along with new broad signals tentatively assigned as **7**. Low temperature ^{1}H NMR spectroscopy was performed on this sample, but did not de-coalesce these broad peaks. Due to this, attempts to isolated **7** were unsuccessful. However, a single discrete complex was isolated from the addition of one equiv of benzyl potassium to **2** (**Figure 9**). Based on ^{1}H NMR, this complex was determined to be **10**. Single crystals of **10** suitable for X-Ray diffraction were grown from a concentrated THF solution with pentane vapour diffusion that was then stored at -35°C for 3 days. The structure of **10** shows that the benzyl substituent is cis to the central N of the redox-active ligand with two THF ligands bound to Y. The potassium counter cation is situated between the aromatic ring of the benzyl substituent and an N-C-C-N moiety of the redox-active ligand. The distances from K to the aryl ring and ligand range from 3.154 to 3.258 and 3.005 to 3.041 Å, which are consistent with pi cation interactions.[31] The C-C and C-N bond distances in **10** are consistent with C-C double bonds and C-N single bonds, ranging from 1.378 to 1.449 and 1.377 to 1.412 Å respectively, which indicates the ligand is in a reduced state.

Complex **10** was used in order to probe the C-C bond forming step in the proposed mechanism for cross-coupling catalyzed by **2** (**Figure 9b**). Addition of one equiv of (1-bromoethyl)benzene to **10** results in the formation of the cross-coupled product (80%) and minor amounts of homocoupled electrophile. A new metal complex is also observed in the ^{1}H NMR spectrum from this reaction, indicated by a new set of aromatic peaks and a new TMS peak. This new species is tentatively assigned as **11**. This assignment was made based on a stoichiometric reaction where tetrabutylammonium bromide was added to **2**, which resulted in the formation of a new species with similar chemical shifts (see Supporting Information, Figure S39). Attempts to crystallize **11** over multiple days resulted in the isolation of **2**, likely through the elimination of KBr. Complex **10** was also tested as a catalyst under our standard conditions and was found to be a competent catalyst for the cross-coupling of (1-bromoethyl)benzene with benzyl zinc bromide (**Figure 9c**).

EPR spectroscopy was also used to further probe the intermediacy of radicals in the catalytic cross-coupling of (1-bromoethyl)benzene with benzyl zinc bromide using 10 mol% **2** (**Figure 10**). We propose that during catalysis the paramagnetic complex **8** and a benzylic radical intermediate form. An EPR spectrum taken on a sample of **2** with 10 equiv of benzyl zinc bromide shows no signal, whereas an EPR spectrum taken on a sample where (1-bromoethyl)benzene was added to the sample of **2** with 10 equiv of benzyl zinc bromide shows a signal (Figure S40). Low temperature EPR spectroscopy was also performed on this sample (Figure S41). A simulation with good agreement to the experimental spectrum consists of two species with g_1 = 1.9819 (weight = 0.7868, linewidth = 2.7451) and g_2 = 1.9863 (weight = 0.3026, linewidth = 6.3454). This data supports radical formation in catalysis.

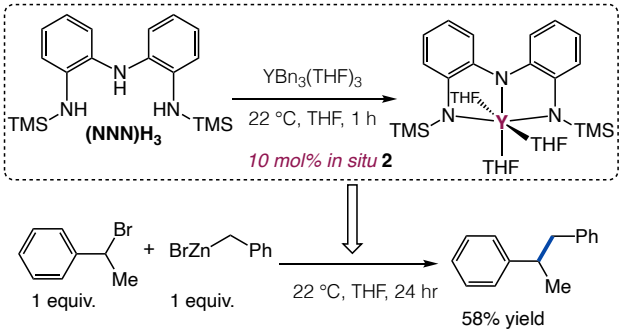

Figure 10. Catalyst formation in situ followed by catalytic cross-coupling

To demonstrate the convenience of late-stage catalyst optimization, this catalytic reaction also worked when the catalyst was generated *in situ*. Addition of $(NNN)H_3$ to YBn_3THF_3 in THF-d_8 to generate complex **2** prior to the addition of 10 equiv. of benzyl zinc bromide and (1-bromoethyl)benzene (representing 10 mol% of catalyst **2**) resulted in the consumption of 58% of the starting materials after 24 h (**Figure 10**) (See Supporting Information, Figure S42 for reaction monitoring comparison to isolated **2**).

Expansion of Scope through mechanistic understanding:

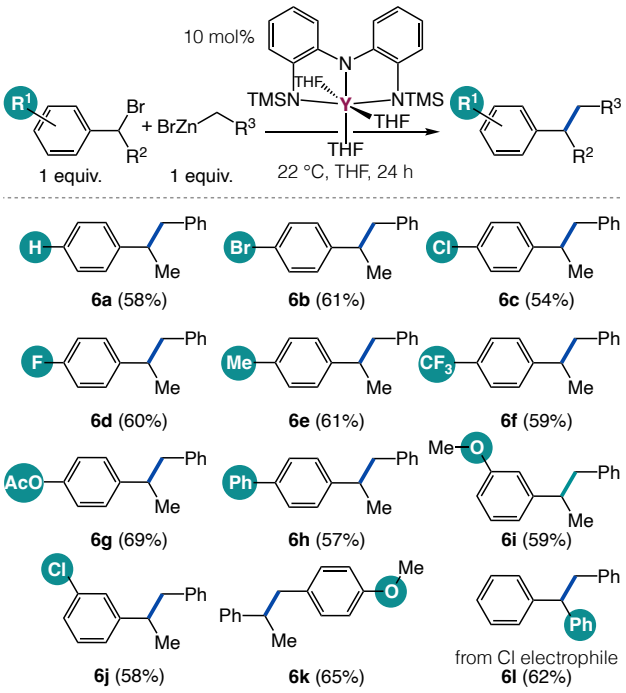

Figure 11. Expanded scope and efficiency, yields calculated by NMR spectroscopy using an internal standard

Cross-coupled products were formed in yields ranging from 54-69% in 24 h (**Figure 11**). This is in stark contrast to the scope with **1** which needed much longer reaction times (up to 4 days). It should be noted that all but one of these products contain β-hydrogens. Similar to our previous report, complex **2** is selective for cross-coupling of alkyl bromides versus aryl bromides as demonstrated by **6b**. This system is also compatible with the presence alkyl fluoride bonds as shown with **6f**. Products **6g**, **6i** and **6k**, that contain -OMe and -OAc, demonstrate that Lewis basic functional groups are tolerated in this catalysis. In particular, **6i** and **6k** demonstrate that Lewis basic functional groups in the electrophile and nucleophile are tolerated. Products **6i** and **6j** show that this system is compatible with *meta*-substituted substrates. In order to further investigate expanding the scope of this reaction, we also explored other halide electrophiles as well as non-benzylic

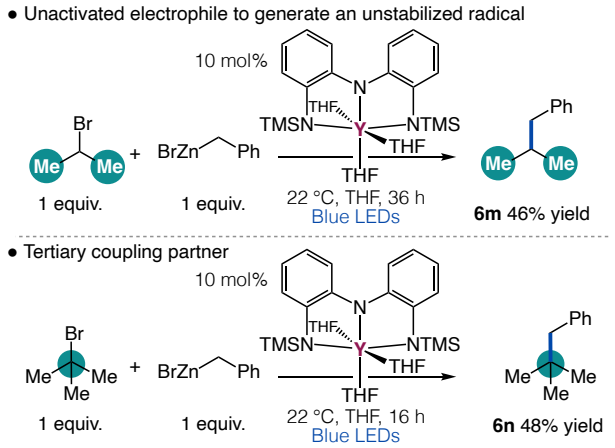

Figure 12. Access to challenging substrates enabled through light

substrates. No product was observed when (1-chloroethyl)benzene was used. But chlorodiphenylmethane was successfully employed as an electrophile to form **6l**, which demonstrates that alkyl chlorides can be used in this alkyl-alkyl cross-coupling. Isopropyl bromide was explored as an electrophile for a non-benzylic substrate, but no cross-coupled product formed. The more activated isopropyl io

dide did not work as well.

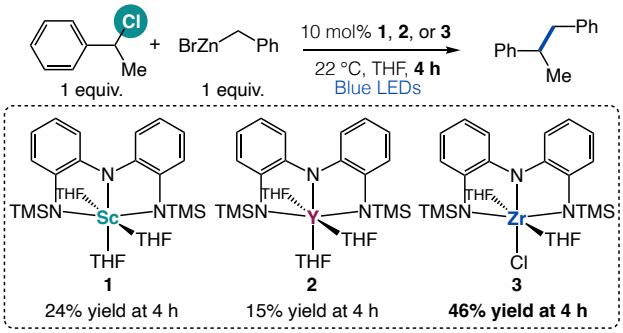

Figure 13. Metal tuning for optimized reactivity

Given the importance of oxidation potentials for the activity of our catalyst system, as well as the precedent for photoreductants, we hypothesized that employing light with **2** would allow challenging and unactivated substrates to be used in our reaction.[32,33] Unactivated substrate isopropyl bromide, which would yield unstablized isopropyl radical, resulted in the complete consumption of isopropyl bromide after 36 h to give a 47% yield of cross-coupled product **6m**. Unactivated tertiary electrophiles are challenging substrates in traditional cross-coupling. Thus to further investigate the applicability of these photocatalytic conditions, *tert*-butyl bromide was also tested as an electrophile. Under these conditions the cross-coupled product **6n** was formed in 48% yield. Presumably, photoexcitation of **2** generates a more potent reductant that allows for the activation of more challenging alkyl halides.

We hypothesized that metal tuning could be employed to further improve reactions catalyzed by **1**, **2**, or **3** and light by potentially reversing the trends seen without light. Therefore we used the benzylic system used in the mechanistic studies as a model substrate but as the more challenging chloride variant that did not perform in reactions without light (**Figure 13**). Although all catalysts went to full conversion of starting material by 24 h, interestingly, the Zr complex **3** performed the best with a 46% yield of cross-coupled product compared to the 24% and 15% yields with **1** and **2** respectively at 4 h. This demonstrates that **3**, with its highest oxidation potential, can be enabled by light to be an efficient catalyst. This exciting result is being further explored in our laboratory.

Metal tuning can be used to improve and expand the scope of early transition metal-catalyzed cross coupling. By understanding the mechanism of the reaction, which proceeds through radical intermediates, the ideal metal can be chosen in order to optimize the reaction. Due to its low oxidation potential as determined by CV, the Y complex **2** was the most favorable catalyst for this reaction. A wide functional group tolerance was demonstrated as well as the use of unactivated and challenging substrates was shown. Ultimately, these studies led to the development of a room temperature early transition metal-catalyzed alkyl–alkyl bond forming reaction.

ASSOCIATED CONTENT

Supporting Information

The Supporting Information is available free of charge on the ACS Publications website.

Experimental (PDF)
Crystal structures can be found in the CCDC:
2121229, 2175190, and 2175196

AUTHOR INFORMATION

Corresponding Author

*Courtney C. Roberts, Department of Chemistry, University of Minnesota, Minneapolis, MN, 55455, United Sates
orcid.org/0000-0001-8177-4013; Email: ccrob@umn.edu

Authors

Roman G. Belli − Department of Chemistry, University of Minnesota, Minneapolis, Minnesota 55455, United States;

orcid.org/0000-0001-6146-670X

Victoria C. Tafuri − Department of Chemistry, University of Minnesota, Minneapolis, Minnesota 55455, United States;

orcid.org/0000-0003-1486-2018

Author Contributions

All authors have given approval to the final version of the manuscript.

Funding Sources

Financial support was provided by the University of Minnesota and the Petroleum Research Fund of the American Chemical Society (ACS PRF 62432-DNI1).

Notes

The authors declare no competing financial interest.

ACKNOWLEDGMENT

We acknowledge the Tonks and Lu groups for equipment use to obtain CV and UV−vis data. X-ray diffraction experiments were performed using a crystal diffractometer acquired through an NSF-MRI award (CHE-1229400) in the X-ray laboratory supervised by Dr. Victor G. Young, Jr. We gratefully acknowledge Chris Seong for help in figure preparation.

REFERENCES

(1) Hedström, A.; Izakian, Z.; Vreto, I.; Wallentin, C.-J.; Norrby, P.-O. On the Radical Nature of Iron-Catalyzed Cross-Coupling Reactions. *Chemistry – A European Journal* **2015**, *21* (15), 5946–5953. https://doi.org/10.1002/chem.201406096.

(2) Cassani, C.; Bergonzini, G.; Wallentin, C.-J. Active Species and Mechanistic Pathways in Iron-Catalyzed C–C Bond-Forming Cross-Coupling Reactions. *ACS Catal.* **2016**, *6* (3), 1640–1648. https://doi.org/10.1021/acscatal.5b02441.

(3) Campeau, L.-C.; Hazari, N. Cross-Coupling and Related Reactions: Connecting Past Success to the Development of New Reactions for the Future. *Organometallics* **2019**, *38* (1), 3–35. https://doi.org/10.1021/acs.organomet.8b00720.

(4) Choi, J.; Fu, G. C. Transition Metal–Catalyzed Alkyl-Alkyl Bond Formation: Another Dimension in Cross-Coupling Chemistry. *Science* **2017**, *356* (6334), eaaf7230. https://doi.org/10.1126/science.aaf7230.

(5) Diccianni, J. B.; Diao, T. Mechanisms of Nickel-Catalyzed Cross-Coupling Reactions. *Trends in Chemistry* **2019**, *1* (9), 830–844. https://doi.org/10.1016/j.trechm.2019.08.004.

(6) Thapa, S.; Shrestha, B.; Gurung, S. K.; Giri, R. Copper-Catalysed Cross-Coupling: An Untapped Potential. *Org. Biomol. Chem.* **2015**, *13* (17), 4816–4827. https://doi.org/10.1039/C5OB00200A.

(7) Devendar, P.; Qu, R.-Y.; Kang, W.-M.; He, B.; Yang, G.-F. Palladium-Catalyzed Cross-Coupling Reactions: A Powerful Tool for the Synthesis of Agrochemicals. *J. Agric. Food Chem.* **2018**, *66* (34), 8914–8934. https://doi.org/10.1021/acs.jafc.8b03792.

(8) King, A. O.; Yasuda, N. Palladium-Catalyzed Cross-Coupling Reactions in the Synthesis of Pharmaceuticals. In *Organometallics in Process Chemistry*; Brown, J. M., Fürstner, A., Hofmann, P., van Koten, G., Kündig, E. P., Reetz, M., Dixneuf, P. H., Hegedus, L. S., Knochel, P., Murai, S., Abe, A., Series Eds.; Springer Berlin Heidelberg: Berlin, Heidelberg, 2004; Vol. 6, pp 205–245. https://doi.org/10.1007/b94551.

(9) Nicolaou, K. C.; Bulger, P. G.; Sarlah, D. Palladium-Catalyzed Cross-Coupling Reactions in Total Synthesis. *Angewandte Chemie International Edition* **2005**, *44* (29), 4442–4489. https://doi.org/10.1002/anie.200500368.

(10) Johansson Seechurn, C. C. C.; Kitching, M. O.; Colacot, T. J.; Snieckus, V. Palladium-Catalyzed Cross-Coupling: A Historical Contextual Perspective to the 2010 Nobel Prize. *Angewandte Chemie International Edition* **2012**, *51* (21), 5062–5085. https://doi.org/10.1002/anie.201107017.

(11) H., N.-S. S.; R., S. S.; E., B. J.; Ellyn, P.; Tobias, G.; C., J. H.; S., S. M.; G., D. A. Univariate Classification of Phosphine Ligation State and Reactivity in Cross-Coupling Catalysis. *Science* **2021**, *374* (6565), 301–308. https://doi.org/10.1126/science.abj4213.

(12) Börgel, J.; Ritter, T. Late-Stage Functionalization. *Chem* **2020**, *6* (8), 1877–1887. https://doi.org/10.1016/j.chempr.2020.07.007.

(13) Cernak, T.; D. Dykstra, K.; Tyagarajan, S.; Vachal, P.; W. Krska, S. The Medicinal Chemist's Toolbox for Late Stage Functionalization of Drug-like Molecules. *Chemical Society Reviews* **2016**, *45* (3), 546–576. https://doi.org/10.1039/C5CS00628G.

(14) Mashima, K. Diagonal Relationship among Organometallic Transition-Metal Complexes. *Organometallics* **2021**, *40* (21), 3497–3505. https://doi.org/10.1021/acs.organomet.1c00344.

(15) Beaumier, E. P.; Pearce, A. J.; See, X. Y.; Tonks, I. A. Modern Applications of Low-Valent Early Transition Metals in Synthesis and Catalysis. *Nat Rev Chem* **2019**, *3* (1), 15–34. https://doi.org/10.1038/s41570-018-0059-x.

(16) Blackmore, K. J.; Ziller, J. W.; Heyduk, A. F. "Oxidative Addition" to a Zirconium(IV) Redox-Active Ligand Complex. *Inorg. Chem.* **2005**, *44* (16), 5559–5561. https://doi.org/10.1021/ic050997c.

(17) Blackmore, K. J.; Lal, N.; Ziller, J. W.; Heyduk, A. F. Catalytic Reactivity of a Zirconium(IV) Redox-Active Ligand Complex with 1,2-Diphenylhydrazine. *J. Am. Chem. Soc.* **2008**, *130* (9), 2728–2729. https://doi.org/10.1021/ja710611v.

(18) Munhá, R. F.; Zarkesh, R. A.; Heyduk, A. F. Tuning the Electronic and Steric Parameters of a Redox-Active Tris(Amido) Ligand. *Inorg. Chem.* **2013**, *52* (19), 11244–11255. https://doi.org/10.1021/ic401496w.

(19) Nguyen, A. I.; Blackmore, K. J.; Carter, S. M.; Zarkesh, R. A.; Heyduk, A. F. One- and Two-Electron Reactivity of a Tantalum(V) Complex with a Redox-Active Tris(Amido)

Ligand. *J. Am. Chem. Soc.* **2009**, *131* (9), 3307–3316. https://doi.org/10.1021/ja808542j.

(20) Broere, D. L. J.; Plessius, R.; Vlugt, J. I. van der. New Avenues for Ligand-Mediated Processes – Expanding Metal Reactivity by the Use of Redox-Active Catechol, o-Aminophenol and o-Phenylenediamine Ligands. *Chem. Soc. Rev.* **2015**, *44* (19), 6886–6915. https://doi.org/10.1039/C5CS00161G.

(21) Lyaskovskyy, V.; de Bruin, B. Redox Non-Innocent Ligands: Versatile New Tools to Control Catalytic Reactions. *ACS Catal.* **2012**, *2* (2), 270–279. https://doi.org/10.1021/cs200660v.

(22) Myers, T. W.; Yee, G. M.; Berben, L. A. Redox-Induced Carbon–Carbon Bond Formation by Using Noninnocent Ligands. *European Journal of Inorganic Chemistry* **2013**, *2013* (22–23), 3831–3835. https://doi.org/10.1002/ejic.201300192.

(23) Belli, R. G.; Tafuri, V. C.; Joannou, M. V.; Roberts, C. C. D0 Metal-Catalyzed Alkyl–Alkyl Cross-Coupling Enabled by a Redox-Active Ligand. *ACS Catalysis* **2022**, *12* (5), 3094–3099. https://doi.org/10.1021/acscatal.1c06002.

(24) Elgrishi, N.; Rountree, K. J.; McCarthy, B. D.; Rountree, E. S.; Eisenhart, T. T.; Dempsey, J. L. A Practical Beginner's Guide to Cyclic Voltammetry. *J. Chem. Educ.* **2018**, *95* (2), 197–206. https://doi.org/10.1021/acs.jchemed.7b00361.

(25) Burés, J. A Simple Graphical Method to Determine the Order in Catalyst. *Angewandte Chemie International Edition* **2016**, *55* (6), 2028–2031. https://doi.org/10.1002/anie.201508983.

(26) Burés, J. Variable Time Normalization Analysis: General Graphical Elucidation of Reaction Orders from Concentration Profiles. *Angewandte Chemie International Edition* **2016**, *55* (52), 16084–16087. https://doi.org/10.1002/anie.201609757.

(27) Nielsen, C. D.-T.; Burés, J. Visual Kinetic Analysis. *Chemical Science* **2019**, *10* (2), 348–353. https://doi.org/10.1039/C8SC04698K.

(28) Blackmond, D. G. Reaction Progress Kinetic Analysis: A Powerful Methodology for Mechanistic Studies of Complex Catalytic Reactions. *Angew Chem Int Ed Engl* **2005**, *44* (28), 4302–4320. https://doi.org/10.1002/anie.200462544.

(29) Blackmond, D. G. Kinetic Profiling of Catalytic Organic Reactions as a Mechanistic Tool. *Journal of the American Chemical Society* **2015**, *137* (34), 10852–10866. https://doi.org/10.1021/jacs.5b05841.

(30) Creary, X. Super Radical Stabilizers. *Acc. Chem. Res.* **2006**, *39* (10), 761–771. https://doi.org/10.1021/ar0680724.

(31) Dougherty, D. A. The Cation−π Interaction. *Acc. Chem. Res.* **2013**, *46* (4), 885–893. https://doi.org/10.1021/ar300265y.

(32) Targos, K.; Williams, O. P.; Wickens, Z. K. Unveiling Potent Photooxidation Behavior of Catalytic Photoreductants. *Journal of the American Chemical Society* **2021**, *143* (11), 4125–4132. https://doi.org/10.1021/jacs.1c00399.

(33) Tay, N. E. S.; Lehnherr, D.; Rovis, T. Photons or Electrons? A Critical Comparison of Electrochemistry and Photoredox Catalysis for Organic Synthesis. *Chemical Reviews* **2022**, *122* (2), 2487–2649. https://doi.org/10.1021/acs.chemrev.1c00384.

Metal Tuning: *simple and efficient 1-step catalyst tuning*